

Elastic scattering of electrons from tetrahydrofurfuryl alcohol

A.R. Milosavljević^{1,a}, F. Blanco², D. Šević¹, G. García³, and B.P. Marinković¹

¹ Institute of Physics, Pregrevica 118, 11080 Belgrade, Serbia and Montenegro

² Departamento de Física Atómica Molecular y Nuclear, Facultad de Ciencias Físicas, Universidad Complutense, Avda. Complutense s/n, 28040 Madrid, Spain

³ Instituto de Matemáticas y Física Fundamental, Consejo Superior de Investigaciones Científicas, Serrano 121, 28006 Madrid, Spain

Received 27 March 2006 / Received in final form 5 May 2006

Published online 15 June 2006 – © EDP Sciences, Società Italiana di Fisica, Springer-Verlag 2006

Abstract. Differential cross-sections (DCSs) for elastic scattering of electrons from tetrahydrofurfuryl alcohol (THFA), which can be considered as an analogue molecule to DNA sugar deoxyribose, were determined using crossed beam measurements for incident energies from 40 eV to 300 eV and scattering angles from 30° to 110°. The relative DCSs were measured both as a function of incident electron energy and scattering angle, allowing absolute calibration of the whole data set via normalization to a single point. The absolute calibration has been performed according to calculated absolute DCSs obtained by the corrected independent atom method using an improved quasifree absorption model. The calculated data-set includes DCSs and integral elastic and inelastic cross-sections in the incident energy range from 5 eV to 5000 eV. The theoretical results agree very well with the experimental ones, regarding the shape of DCSs. Moreover, the same theoretical procedure has been used to obtain DCSs for elastic electron scattering from a simpler deoxyribose analogue tetrahydrofuran (THF), which agree very well, both in shape and on the absolute scale, with the recent experimentally obtained absolute DCSs [A.R. Milosavljević et al., Eur. Phys. J. D **35**, 411 (2005)]. The present results are also compared with the recent theoretical data for THF and THFA. Finally, according to both experimental and theoretical data, the DCSs for elastic electron scattering from THFA and THF molecules appear to be very similar both in shape and absolute scale.

PACS. 34.80.Bm Elastic scattering of electrons by atoms and molecules – 34.10.+x General theories and models of atomic and molecular collisions and interactions

1 Introduction

The investigation of electron interaction with molecules that represent the DNA components has been motivated in recent years by a need for understanding the processes that lead to radiation damage of a living cell. It is believed that processes driven by low-energy secondary electrons, which are produced in large quantities on the track of a primary high-energy particle, are of particular importance in a direct DNA damage [1,2]. In this context, a great deal of both experimental and theoretical work on electron interaction with DNA (or RNA) components, namely the bases (adenine, guanine, thymine, cytosine, uracil) and the backbone sugar deoxyribose (or analogue molecules: tetrahydrofuran (THF), tetrahydrofurfuryl alcohol (THFA) and 3-hydroxytetrahydrofuran (3HTHF)), has been reported. A comprehensive review can be found in the recent paper by Leon Sanche [3]. However, only few of these results have been obtained for THFA molecule. Antic et al. [4,5] investigated electron-stimulated desorption yields of H⁻ produced by dissociative electron attachment to THF, THFA and 3HTHF, physisorbed on a

polycrystalline Pt substrate. Very recently, Mozejko and Sanche [6] have calculated differential and integral cross-sections for elastic electron scattering from several selected analogues of components of DNA backbone, including THFA, using the independent atom method with a static-polarization model potential, in the incident electron energy range from 50 eV to 2000 eV. Reliable cross-sections for elastic scattering of electrons from DNA components are of interest in estimating and modelling the by-products production induced by electrons within the molecular sample [7] and are input parameters for energy deposition modelling, which is based on a Monte Carlo simulation of the single scattering process [8–11]. The experimentally obtained absolute DCSs for elastic electron scattering by THF molecule, in the incident energy range from 20 eV to 300 eV and angular range from 10° to 110°, have been reported very recently, as well [12]. However, according to our knowledge, no experimental results concerning electron interaction (neither elastic nor inelastic) with gaseous THFA molecule have been published. A data-set on electron-THFA interaction would give possibilities for investigation of electron-induced decomposition of deoxyribose ring, as well as effects upon

^a e-mail:vrzaz@phy.bg.ac.yu

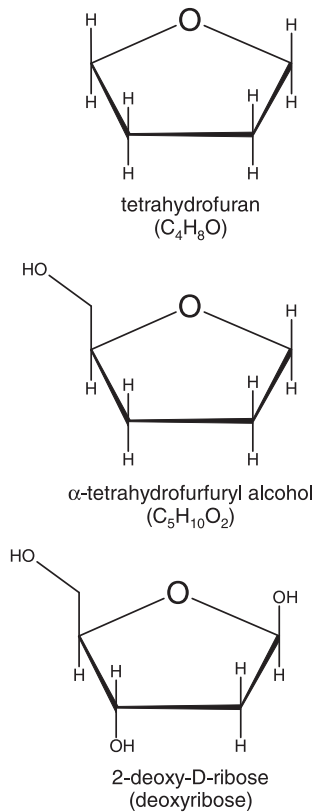


Fig. 1. Schematic drawing of tetrahydrofuran (THF), α -tetrahydrofurfuryl alcohol (THFA) and 2-deoxy-D-ribose (deoxyribose) molecules.

substitution of α -H atom in THF by the $-\text{CH}_2\text{OH}$ group and, hence, the applicability of results obtained for the simplest THF analogue to describe electron-deoxyribose interaction. The structural formulae of the deoxyribose, THFA and THF molecules are given in Figure 1.

In the present paper, we report both theoretical and experimental results on elastic electron interaction with THFA molecule. The experimental absolute normalized DCSs are obtained in small energy and angular steps, in the incident energy range from 40 eV to 300 eV and angular range from 30° to 110° . The calculations of DCSs and integral elastic and inelastic cross-sections are based on the independent atom method (IAM) [13], with an improved quasifree absorption model potential, which includes relativistic and many-body effects, as well as non-ionization inelastic processes [14]. The theoretical results are obtained in the incident energy range from 5 eV to 5000 eV and agree very well with the available experimental data. Finally, both theoretical and experimental results for THFA molecule are compared to corresponding THF data.

2 Experiment

A detailed description of the experimental set-up and a discussion of the measurement procedure for obtaining DCSs as a function of either scattering angle or incident

electron energy, has been given recently [15]. Briefly, an electron gun produces a nonmonochromated, well collimated incident electron beam, which is crossed perpendicularly by a molecular beam produced by a stainless still needle. The gun can be rotated around the needle in the angular range from about -40° to 120° . The scattered electrons are retarded and focused by a four-element cylindrical electrostatic lens into a double cylindrical mirror analyzer, followed by three-element focusing lens and a single channel electron multiplier. The base pressure of about 4×10^{-7} mbar was obtained by a turbo-molecular pump. The working pressure was usually less than 5×10^{-6} mbar and was checked for each experimental point. The uncertainty of the incident energy scale was determined to be less than ± 0.4 eV, by observing a threshold for He^+ ions yield. The best energy resolution was about 0.4 eV (limited by thermal spread of primary electrons). However, the resolution was lowered (1–1.5 eV) for measurements of DCSs as a function of incident electron energy in order to reduce energy dependence of the transmission function (see [15]). It should be noted that even with the best applied resolution, the present elastic DCSs inevitably include rotational and vibrational excitations. The latter, however, should not distort significantly elastic DCSs at the presented incident energies, as was discussed in the previous paper [12]. The angular resolution was determined to be better than $\pm 2^\circ$. The experimental procedure was checked according to benchmark DCSs for elastic electron scattering by Kr, as a function of both scattering angle and incident electron energy, which were measured directly before and after electron-THFA measurements. The anhydrous THFA was purchased from Merck KGaA with a declared purity of $>98\%$ and was used after several cycles of freeze-thaw under vacuum. Because of a rather low vapor pressure of THFA (more than two orders of magnitude lower at 20°C than that of THF [16]), the sample container was heated during a measurement at the temperature of about 70°C .

The whole set of relative DCSs, i.e. the relative surface $\text{DCS} = f(E_0, \theta)$, which has been obtained by independent DCS measurements both as a function of E_0 and θ (see [15]), can be normalized to the absolute scale according to an absolute, referent cross-section value in a single (E_0, θ) point (so, a possible correction to the referent DCS can be then easily applied to the whole data set). To the best of our knowledge, absolute measurements of total, ionization, elastic integral or differential cross-sections, have not been reported so far for THFA molecule. Therefore, the calibration of the present experimental relative data set is performed according to the present theoretical data. The applied theoretical method is confirmed to give reliable absolute integral cross-sections (ICSs) and DCSs for elastic scattering of electrons from different polyatomic molecules, at medium incident electron energies and higher scattering angles above 10° [14]. In particular, the calculations for the similar THF molecule agree very well with the recent absolute experimental data [12] (see Sect. 4). Although a calculated ICS is generally more accurate than an absolute theoretical DCS in a specific (E_0, θ)

point, the calibration to ICS would need an extrapolation of present experimental data which could give even larger uncertainty of the final absolute values. The calibration of the experimental results to the absolute scale has been performed according to the absolute theoretical DCS at 150 eV and 50°. The scattering angle of 50° has been chosen for calibration as giving relatively small normalization errors (the DCSs exhibit a small shoulder near 50°) and still being reasonably distant from DCS minima. Also, the calculations give very good agreement with the experiment in this angular region, regarding the DCS shape. The incident energy of 150 eV has been chosen for calibration according to both the smallest error of the experimental DCS measured as a function of energy at 50° and the smallest variation of theoretical DCS within the angular resolution of the present experiment (see Sect. 4).

The errors for the relative DCSs measured as a function of scattering angle include statistical errors (0.1–3%), according to Poisson's distribution and short-term stability errors (usually 1–5%), according to discrepancy of repeated measurements at the same incident energy and scattering angle. In the case of relative DCSs measured as a function of incident electron energy, the errors due to both instability of incident electron beam (2% to 12%, even 25% for 40 eV) and transmission function (0.5% to 10%) should be accounted, as well (see [15]). The errors of the normalized DCSs account the normalization errors, as well. The latter include both the errors of DCS values measured as a function of incident energy at a fixed scattering angle (discussed above) and an uncertainty of the angular scale, which produces the error that is dependent on the shape of a cross-section at particular incident energy (5% to 6% at the angle of 50°). The final error should also include the uncertainty of the theoretical DCS value used for calibration to the absolute scale.

3 Theoretical method

Present calculations of molecular cross-sections are based on a corrected form of the independent-atom method (IAM), known as the SCAR (Screen Corrected Additivity Rule) procedure. All the details for this procedure have been extensively described in previous works [14, 17] where it was applied to other molecular species, so only a brief comment will be given here.

In the standard IAM approximation the electron-molecule collision is reduced to the problem of collision with individual atoms by assuming that each atom of the molecule scatters independently and that redistribution of atomic electrons due to the molecular binding is unimportant. At low energies, where atomic cross-sections are not small compared to (squared) interatomic distances in the molecule, the IAM approximation fails because the atoms can no longer be considered as independent scatterers and multiple scattering within the molecule is not negligible. These kind of corrections have been revealed as quite important in similar situations [14, 17–20].

It has been shown [14] that the energy range for which deviations from the IAM approximation are relevant de-

pends on the size of the molecule: 10% or larger screening corrections take place for N₂ and CO up to 200 eV, for CO₂ up to 300 eV, and for benzene up to 600 eV.

While the detailed considerations leading to the SCAR expressions are somewhat involved, the final results are relatively simple.

In the first place, for integrated (elastic or inelastic) cross-sections, the usual additivity rule (AR) expressions:

$$\sigma^{total} = \sum_{atoms} \sigma_i, \quad (1)$$

become replaced by modified ones:

$$\sigma^{elastic} = \sum_i s_i \sigma_i^{elastic} \quad \text{and} \quad \sigma^{inelastic} = \sum_i s_i \sigma_i^{inelastic}. \quad (2)$$

Here the introduced screening coefficients ($0 \leq s_i \leq 1$) reduce the contribution from each atom to the total cross-section. Calculation of s_i coefficients requires only data on the position and the total cross-section σ_i of each atom in the molecule. The explicit expressions for s_i are [14, 17]:

$$\begin{aligned} \varepsilon_i^{(1)} &= 1, \\ \varepsilon_i^{(k)} &= \frac{N - k + 1}{N - 1} \sum_{j(\neq i)} \sigma_j \varepsilon_j^{(k-1)} / \alpha_{ij} \quad (k = 2, \dots, N), \end{aligned} \quad (3)$$

$$s_i = 1 - \varepsilon_i^{(2)}/2! + \varepsilon_i^{(3)}/3! - \varepsilon_i^{(4)}/4! + \dots \pm \varepsilon_i^{(N)}/N!. \quad (4)$$

Where N stands for the number of atoms in the molecule, the j index in sums $\sum_{j(\neq i)}$ runs over all the N atoms except the i one, $\alpha_{ij} = \max(4\pi r_{ij}^2, \sigma_i, \sigma_j)$, and r_{ij} is the distance between centers of atoms i and j . The successive auxiliary $\varepsilon_i^{(k)}$ contributions arise from k -atoms overlapping and so only $\varepsilon_i^{(2)}$ exists for diatomics.

Secondly, for the elastic differential cross-section, instead of the standard form

$$\frac{d\sigma^{elastic}}{d\Omega} = \sum_{i,j} f_i(\theta) f_j^*(\theta) \frac{\sin qr_{ij}}{qr_{ij}}, \quad (5)$$

(where, as usual, $q = 2K \sin \theta/2$ is the momentum transfer) now we have [17]

$$\begin{aligned} \frac{d\sigma^{elastic}}{d\Omega} &\cong (1 - X_S) \frac{\sigma^{elastic} - \sigma_D}{4\pi} \\ &+ \left[1 + X_S \left(\frac{\sigma^{elastic}}{\sigma_D} - 1 \right) \right] \frac{d\sigma_D}{d\Omega}, \end{aligned} \quad (6)$$

where σ_D , $d\sigma_D/d\Omega$ and X_S are defined by:

$$\begin{aligned} \sigma_D &= \sum_i s_i^2 \sigma_i^{elastic}, \\ \frac{d\sigma_D}{d\Omega} &= \sum_{ij} s_i s_j f_i(\theta) f_j^*(\theta) \frac{\sin qr_{ij}}{qr_{ij}}, \end{aligned} \quad (7)$$

$$X_S \approx \int_0^{45^\circ} \frac{d\sigma_D}{d\Omega} \sin \theta d\theta / \int_0^{180^\circ} \frac{d\sigma_D}{d\Omega} \sin \theta d\theta. \quad (8)$$

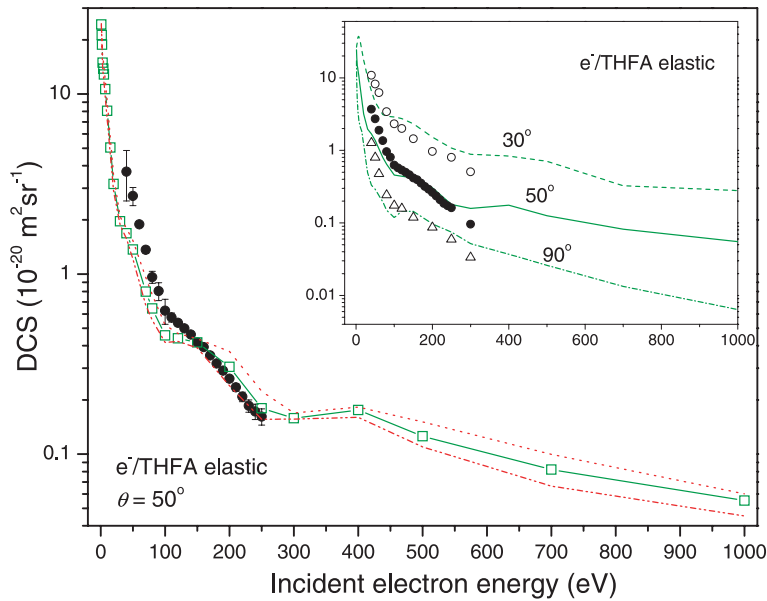


Fig. 2. Energy dependence of absolute DCS for elastic electron scattering from THFA at the scattering angle of 50°: (●), experiment; (□), theory (the DCSs at 48° (···) and 52° (−··) are also given to show a variation of the calculated DCS at a specific incident energy, within the angular region $\pm 2^\circ$). Inset shows experimental and theoretical absolute DCSs versus incident electron energy at the fixed scattering angles of 30° (○, ---), 50° (●, −) and 90° (△, -·-), respectively. The experimental points at 30° and 90° are extracted from the normalized angle-dependent DCSs. The calculated points are connected by straight lines.

Expressions (6–8) resulted in [17] after an analysis of the angular distribution including redispersion processes inside the molecule, and after some estimation on the relevance of these contributions.

It must be noted that only atomic spatial coordinates are necessary for the calculation, with no considerations on molecular symmetry, so the procedure can be easily applied to arbitrary species. Once the atomic cross-sections and dispersion functions are known, the corrected molecular quantities are directly derived from the equations (2), (3), (4), (6), (7) and (8). Screening corrections become very significant only at low energies, resulting in a reduction of total values and a smoothing of maxima and minima for differential ones.

The procedure used for calculation of the corresponding atomic cross-sections has been also extensively described elsewhere [21–23], so only a brief comment will be given here. For our purposes the electron-atom interaction is represented by the approximate ab initio optical potential $V_{opt}(r) = V_s(r) + V_e(r) + V_p(r) + iV^a(r)$. Here $V_s(r)$ is the static potential calculated by using the charge density deduced from Hartree-Fock atomic wave functions including relativistic corrections, $V_e(r)$ is the exchange potential for which the semiclassical energy-dependent formula derived by Riley and Truhlar [24] is used, $V_p(r)$ represents the target polarization potential in the form given by Zhang et al. [25], and finally the absorption potential $V^a(r)$ accounting for inelastic processes is based on the revised quasifree model [21].

For each atom the corresponding radial scattering equation was numerically integrated, and the resulting complex partial wave phase shifts δ_l were used to obtain the atomic scattering amplitudes and total cross-sections [21–23]. In particular, the data used here for C, H, O and N atoms are exactly the same as already used in references [14, 26].

While it is difficult estimating the accuracy of the calculated differential cross-sections, errors larger than 25%

are not to be expected in the 50–500 eV energy range for 30° to 120° angles. This is supported by the observed agreement of this kind of calculations with experimental results for other similar-size molecules (CF₄ and C₃F₈ in [17], or benzene, C₆F₆ and C₄H₈O tetrahydrofuran in [27]).

4 Results and discussion

The DCS for elastic electron-THFA scattering at the angle of 50° is presented in Figure 2. The experimental DCS is directly measured as a function of incident electron energy and normalized to the absolute scale at 150 eV. The error bars of the experimental points also include the uncertainty of the transmission function and the incident electron beam intensity, which are the most significant at the ends of the measured energy range. The theoretical curve is extracted from DCSs tabulated as a function of scattering angle. Theoretical DCSs at 48° and 52° are also shown to present a variation of the calculated DCS at a specific incident energy, within the angular region of $\pm 2^\circ$, which is the lower limit of experimental angular resolution. Generally, there is a good agreement between experimental and theoretical results, both showing a similar behavior of DCS. By using the determined absolute experimental DCS versus incident energy, all the relative DCSs measured as a function of scattering angle, at the incident energies from 50 eV to 250 eV, are normalized to the absolute scale at 50°. The relative DCS at 300 eV has been calibrated to the absolute scale according to the ratio of elastic electron scattering signal at 250 eV and 300 eV, obtained under the same experimental conditions, immediately one after the other at 30°. The absolute DCSs versus incident electron energy, extracted from the normalized angle-dependent DCSs, are compared to the theoretical results at several fixed scattering angles in the inset of Figure 2.

Table 1. Experimentally obtained differential cross-sections for elastic electron scattering from tetrahydrofurfuryl alcohol (THFA) in units of $10^{-20} \text{ m}^2 \text{ sr}^{-1}$ as a function of scattering angle (θ) and incident energy (E_0). The absolute errors (statistical, short-term stability, uncertainty of θ and E_0 , uncertainty of incident electron beam and transmission function) in the last significant digits are given in parentheses. The error due to a variation of the absolute theoretical DCS ($E_0 = 150 \text{ eV}$, $\theta = 50^\circ$), which is used for calibration, within the angular region of $\pm 2^\circ$, is about 11% and should be accounted, as well. The accuracy of the absolute theoretical DCS used for calibration is estimated to be within 25%.

$\theta(^{\circ})$	$E_0 \text{ (eV)}$								
	50	60	80	100	120	150	200	250	300
30	8.2(1.1)	6.24(36)	3.41(33)	2.32(39)	2.00(14)	1.449(84)	0.964(68)	0.802(94)	0.505(81)
35	5.49(71)	4.19(24)	2.46(23)	1.63(27)	1.363(96)	0.899(53)	0.630(45)	0.639(75)	0.378(61)
40	4.18(54)	3.22(18)	1.77(17)	1.11(19)	0.910(64)	0.660(39)	0.523(37)	0.451(53)	0.213(34)
45	3.36(43)	2.48(14)	1.28(12)	0.80(13)	0.649(46)	0.507(30)	0.404(29)	0.251(30)	0.121(19)
50	2.71(35)	1.89(11)	0.962(92)	0.63(11)	0.536(38)	0.417(25)	0.262(19)	0.162(19)	0.096(15)
55	2.12(27)	1.420(82)	0.775(74)	0.545(92)	0.456(33)	0.300(18)	0.170(13)	0.134(16)	0.090(14)
60	1.66(21)	1.152(67)	0.647(62)	0.460(78)	0.346(25)	0.193(12)	0.130(10)	0.124(15)	0.076(12)
65	1.39(18)	0.954(56)	0.575(55)	0.350(59)	0.247(18)	0.1417(90)	0.1247(99)	0.113(13)	0.0606(98)
70	1.14(15)	0.791(47)	0.479(46)	0.262(44)	0.193(14)	0.1203(77)	0.1142(91)	0.098(12)	0.0545(88)
75	1.01(13)	0.710(42)	0.384(37)	0.199(34)	0.156(12)	0.1180(76)	0.1007(82)	0.085(10)	0.0460(74)
80	0.92(12)	0.629(37)	0.307(30)	0.175(29)	0.147(11)	0.1227(79)	0.0976(80)	0.0778(92)	0.0381(62)
85	0.85(11)	0.554(33)	0.272(27)	0.164(28)	0.148(11)	0.1268(81)	0.0902(75)	0.0672(80)	0.0343(55)
90	0.80(10)	0.475(29)	0.242(24)	0.174(29)	0.158(12)	0.1189(77)	0.0867(72)	0.0592(70)	0.0335(54)
95	0.80(10)	0.488(29)	0.256(25)	0.196(33)	0.165(12)	0.1208(78)	0.0792(67)	0.0567(67)	0.0331(53)
100	0.80(10)	0.486(29)	0.298(29)	0.228(38)	0.173(13)	0.1269(81)	0.0714(61)	0.0558(66)	0.0316(51)
105	0.89(12)	0.531(32)	0.370(36)	0.261(44)	0.184(14)	0.1213(78)	0.0709(61)	0.0570(68)	0.0296(48)
110	1.01(13)	0.611(36)	0.423(41)	0.297(50)	0.200(15)	0.1285(82)	0.0749(64)	0.058(68)	0.0284(46)

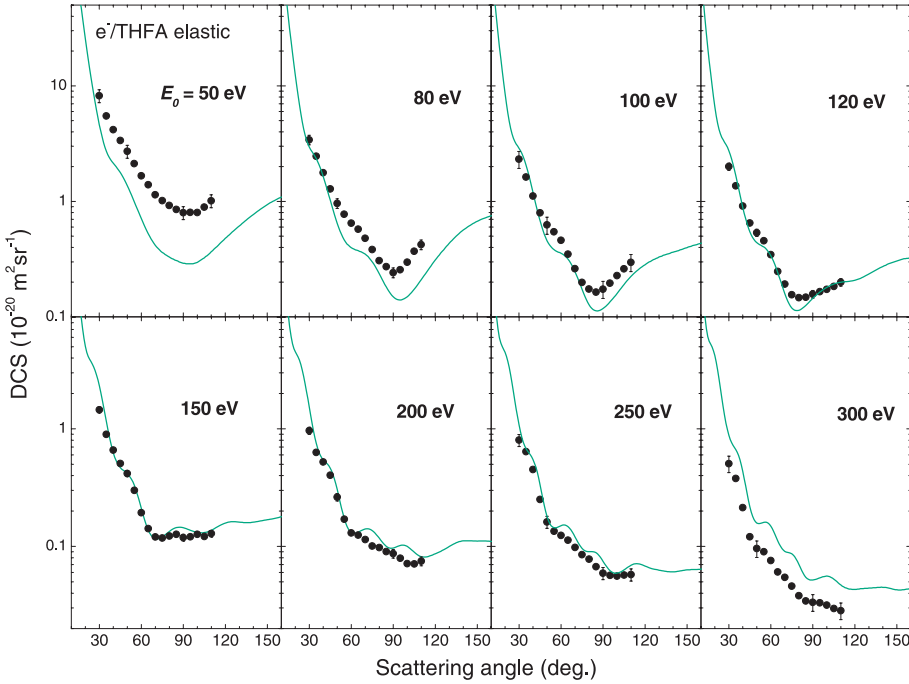


Fig. 3. Angular dependence of absolute DCSs for elastic electron scattering from THFA molecule at different incident energies: (●), experiment; (—), theory.

The experimental absolute DCSs as a function of the scattering angle are obtained for the incident electron energies of 50, 60, 80, 100, 120, 150, 200, 250 and 300 eV, in the angular range from 30° to 110° , in 5° steps. The results are presented in Table 1. The DCSs at chosen incident energies are presented in Figure 3, as well as the absolute theoretical DCSs. Generally, the theoretical results agree very well with the experiment. A disagreement between absolute magnitudes at the lowest (50 eV) and

the highest (300 eV) presented incident energies emerges as a consequence of the disagreement between relative behavior of theoretical and experimental DCSs versus incident energy at 50° (Fig. 2), the latter being used for the calibration to the absolute scale. However, a very good agreement of a relative behavior of DCS versus scattering angle can be seen at all presented energies. The DCSs at lower incident energies are characterized by a rather broad minimum at about 90° , which slowly disappears

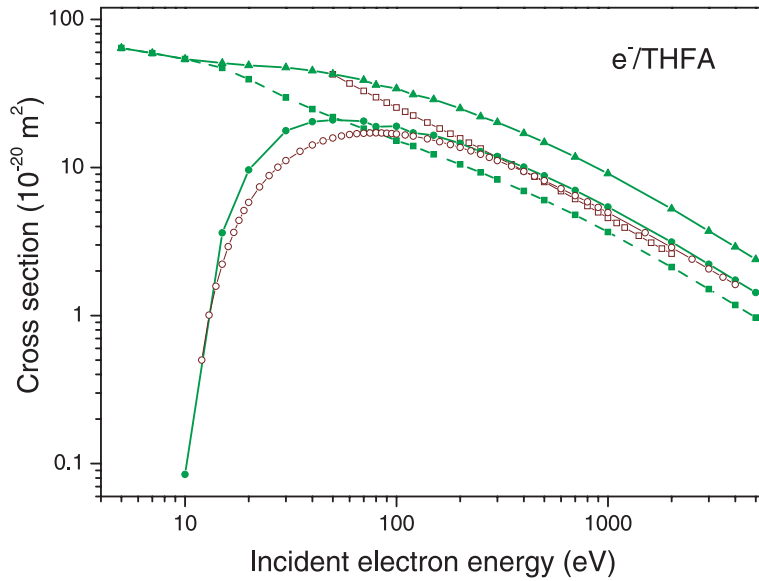


Fig. 4. Calculated integral elastic cross-section (—■—, present; —□—, [6]), integral inelastic cross-section (—●—, present), total cross-section for single ionization (—○—, [6]) and total cross-section (—▲—, present) for electron scattering from THFA molecule.

Table 2. Calculated integral elastic and inelastic and total cross-sections for electron scattering from tetrahydrofurfuryl alcohol (THFA) in units of 10^{-20} m^2 as a function of incident energy (E_0).

E_0 (eV)	Elastic	Inelastic	Total
5	64.12	0.000	64.12
7	59.08	0.000	59.08
10	54.04	0.08456	54.04
15	47.04	3.612	50.68
20	39.48	9.632	49.00
30	29.68	17.72	47.32
40	24.78	20.36	45.08
50	21.87	20.94	42.84
70	18.26	20.55	38.92
80	17.36	18.90	36.12
100	15.18	18.98	34.16
120	13.94	17.14	31.08
150	12.26	16.49	28.84
200	10.50	14.56	25.06
250	9.268	12.80	22.06
300	8.288	11.87	20.19
400	6.944	10.05	17.00
500	6.020	8.792	14.78
700	4.788	7.000	11.79
1000	3.668	5.404	9.100
2000	2.122	3.136	5.264
3000	1.509	2.220	3.724
4000	1.179	1.736	2.912
5000	0.969	1.428	2.397

with increasing the electron energy above 120 eV. In the energy range from 50 eV to 300 eV, the absolute DCSs decrease for more than order of magnitude. In Table 2 and Figure 4, the present calculated integral elastic, inelastic and total cross-sections for electron scattering from THFA molecule are given. The recent theoretical results by Mozejko and Sanche [6], obtained by IAM with a static-polarization model potential, are presented, as well. The

latter calculations give higher integral elastic cross-section with somewhat different slope. However, the ionization cross-section, given in the same paper [6], agrees very well with the present integral inelastic cross-sections, except in the energy region from about 15 eV to 90 eV where the present calculation, which also includes excitation processes, logically gives higher values.

In Figure 5, the present absolute DCSs for elastic electron-THFA scattering at 50 eV, 100 eV and 200 eV are compared with the recent absolute theoretical DCSs [6], as well as with the absolute experimental [12] and theoretical [6] DCSs for elastic electron-THF scattering. The experimental DCSs for THF are somewhat lower on the absolute scale, which is to be expected considering sizes of the molecules. At the energy of 50 eV, this difference is more significant for experimental DCSs, which could be also a consequence of the normalization procedure, i.e. the uncertainty of the incident electron beam intensity at the end of the covered energy interval (see [15]). Nevertheless, the disagreement between different theoretical methods is also the most significant at the lowest presented energy. Therefore, absolute measurements on elastic electron-THFA scattering are needed to clear this out. At higher medium incident energies, the experimental results show that DCSs for electron-THF and THFA scattering are very similar, both in shape and on the absolute scale. This is also confirmed by both sets of theoretical results, which agree well with the experiment. However, the present theoretical method is clearly superior, considering both the absolute magnitudes and the shapes of DCSs for both molecules.

5 Conclusion

The elastic scattering of electrons from tetrahydrofurfuryl alcohol (THFA) has been investigated, both experimentally and theoretically. The measurements were performed

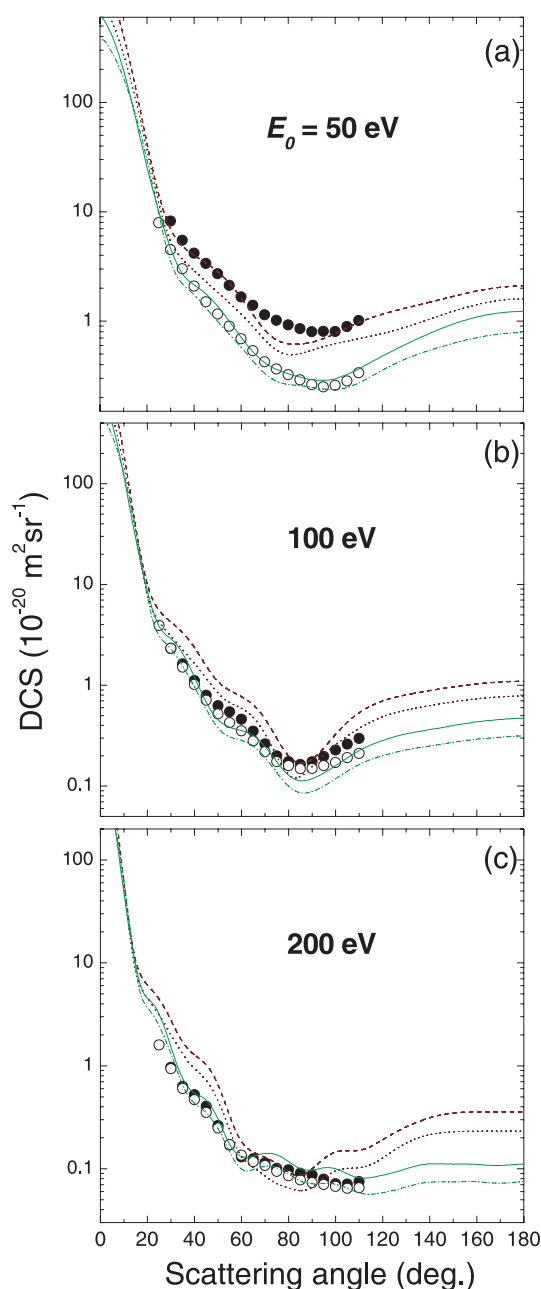


Fig. 5. Absolute DCSs for elastic electron scattering from different molecules at the incident energies of 50 eV, 100 eV and 200 eV: (●), THFA present experiment; (○), THF experiment [12]; (—), THFA present theory; (---), THF present theory; (---), THFA theory [6]; (···), THF theory [6].

using a cross-beam experiment, for the incident electron energies from 40 eV to 300 eV and scattering angles from 30° to 110°. The relative DCSs were measured independently as a function of both incident energy and scattering angle. The calibration to the absolute scale has been obtained according to the present theoretical results. The latter calculations were based on a corrected form of the independent-atom method, known as the Screen Corrected Additivity Rule procedure, using an approximate

ab initio model potential known as the quasifree absorption model, which is improved to correct for many-body effects and nonionization processes.

The shape of the present experimental DCSs for elastic electron-THFA scattering, as well as of the recently published experimental DCSs for elastic electron-THF scattering [12], is very well reproduced by the present calculations. Therefore, at least in the angular range from about 20° to 120°, the latter can be used for reasonable and fast estimation of the DCSs for elastic scattering of electrons by DNA deoxyribose analogue molecules. The behavior of the DCSs still need to be investigated in the forward and the backward scattering direction, where further experimental measurement are needed, as well as at low incident electron energies.

The elastic DCSs for THF and THFA molecules appear to be rather similar, both in shape and on the absolute scale, especially at higher intermediate incident energies above 80 eV. This means that a substitution of the α -H atom of the THF molecule by the $-\text{CH}_2\text{OH}$ group does not affect significantly an elastic scattering process in this incident energy region. Therefore, the behavior of the DCSs for elastic THF and THFA scattering, as well as their absolute magnitudes, can be used for a good estimation of elastic electron interaction with the DNA sugar deoxyribose. The presented set of tabulated absolute DCSs and ICSs for electron scattering by THFA is then useful for further modelling of low(medium) electron interaction with large biomolecules, such as DNA, RNA, virus inhibitors etc.

We are very grateful to Dr Pawel Mozejko from Gdansk University of Technology for sending us calculated results in numerical form, as well as for useful discussion. This work has been partially supported by Ministry of Science and Environmental Protection of Republic of Serbia under project 141011 and the Spanish Ministerio de Educacion y Ciencia (Project BFM2003-04648/FISI) and motivated by research within COST Action P9 “Radiation Damage in Biomolecular Systems”.

References

1. D. Michael, P. O’Neil, *Science* **287**, 1603 (2000)
2. B. Boudaiffa, P. Cloutier, D. Hunting, M.A. Huels, L. Sanche, *Science* **287**, 1658 (2000)
3. L. Sanche, *Eur. Phys. J. D* **35**, 367 (2005)
4. D. Antic, L. Parenteau, M. Lepage, L. Sanche, *J. Phys. Chem. B* **103**, 6611 (1999)
5. D. Antic, L. Parenteau, L. Sanche, *J. Phys. Chem. B* **104**, 4711 (2000)
6. P. Mozejko, L. Sanche, *Radiat. Phys. Chem.* **73**, 77 (2005)
7. S.-P. Breton, M. Michaud, C. Jäggle, P. Swiderek, L. Sanche, *J. Chem. Phys.* **121**, 11240 (2004)
8. A. Roldán, J.M. Pérez, A. Williard, F. Blanco, G. Garcia, *J. Appl. Phys.* **95**, 5865 (2004)
9. V.A. Semenko, J.E. Turner, T.B. Borak, *Radiat. Environ. Biophys.* **42**, 213 (2003)
10. U. Titt, V. Dangendorf, B. Grosswendt, H. Schuhmacher, *Nucl. Instr. Meth. A* **477**, 536 (2002)

11. W. Friedland, P. Jacob, H.G. Paretzke, M. Marzagora, A. Ottolenghi, *Radiat. Environ. Biophys.* **38**, 39 (1999)
12. A.R. Milosavljević, A. Giuliani, D. Šević, M.-J. Hubin-Franskin, B.P. Marinković, *Eur. Phys. J. D* **35**, 411 (2005)
13. N.F. Mott, H.S.W. Massey, *The theory of atomic collisions*, 3rd edn. (Clarendon Press, Oxford, 1971)
14. F. Blanco, G. García, *Phys. Lett. A* **317**, 458 (2003)
15. A.R. Milosavljević, S. Madžunkov, D. Šević, I. Čadež, B.P. Marinković, *J. Phys. B: At. Mol. Opt. Phys.* **39**, 609 (2006)
16. The Merck Chemical Databases (<http://chemdat.merck.de>)
17. F. Blanco, G. García, *Phys. Lett. A* **330**, 230 (2004)
18. K.N. Joshipura, P.M. Patel, *J. Phys. B: At. Mol. Opt. Phys.* **29**, 3925 (1996)
19. Y. Jiang, J. Sun, L. Wan, *J. Phys. B: At. Mol. Opt. Phys.* **30**, 5025 (1997); Y. Jiang, J. Sun, L. Wan, *Phys. Rev. A* **62**, 062712 (2000)
20. A. Zecca, R. Melissa, R. Brusa, G. Karwasz, *Phys. Lett. A* **257**, 75 (1999)
21. D.R. Penn, *Phys. Rev. B* **35**, 482 (1987)
22. F. Blanco, G. García, *Phys. Lett. A* **255**, 147 (1999)
23. F. Blanco, G. García, *Phys. Lett. A* **295**, 178 (2002)
24. M.E. Riley, D.G. Truhlar, *J. Chem. Phys.* **63**, 2182 (1975)
25. X.Z. Zhang, J.F. Sun, Y.F. Liu, *J. Phys. B: At. Mol. Opt. Phys.* **25**, 1893 (1992)
26. F. Blanco, G. García, *Phys. Rev. A* **67**, 022701 (2003)
27. F. Blanco, G. García, *Phys. Lett. A* (submitted)